Infrared Photometry for Near-Earth Objects From Spitzer – the Full Sample

A.J. McNeill[1], A. Allen[2], J.L. Hora[3], D.E. Trilling[2] and H. Smith[3]

[1]Department of Physics and Astronomy, Bowling Green State University, 806 Ridge St, Bowling Green, OH 43403; USA

[2]Department of Astronomy and Planetary Science, Northern Arizona University, Flagstaff, AZ 86011, USA

[3]Center for Astrophysics, Harvard Smithsonian, 60 Garden Street, MS-65, Cambridge, MA 02138-1516; USA

Abstract

The IRAC camera on the Spitzer Space Telescope observed 2175 Near Earth Objects (NEOs) during its Warm Mission phase, across three large surveys and a small number of dedicated small projects. We present the final reprocessing of the NEO data and infrared photometry in the 3.6 μm and 4.5 μm regimes [1]. The window of observation has allowed for a small number of complete light curves to be constructed along with a greater number of partial light curves. For those objects for which we have full light curves we determine period and amplitude.

Additionally we use the full sample of partial light curves to update our estimated shape distribution for Near Earth Objects from prior studies [2] for better comparison with upcoming work to determine the shape distribution of main-belt asteroids of similar size. By combining Spitzer infrared photometry with optical photometry from PanSTARRS we also present improved albedo and diameter estimates for objects observed during the same period using the Near-Earth Asteroid Thermal Model (NEATM) [3]. These results are of great relevance to planetary defense as shape, strength, size and spin are key parameters when planning defense measures.

The Spitzer NEO Sample

We present a full reprocessing of all near-Earth object (NEO) observations from the Spitzer Space Telescope's Warm Mission, yielding the definitive infrared flux and lightcurve catalog

- **2175 unique NEOs** observed with IRAC across 2432 observing epochs in the 3.6 μm and 4.5 μm wavelength ranges.
- **39 NEOs** with complete lightcurve coverage and accurately determined periods sampled across multiple rotations.
- **A further 128 NEOs** with sufficient lightcurve coverage for lower limits on period and amplitude.
- **11 candidate SFRs** with a combination of rotation period and elongation requiring internal cohesive strength to resist rotational fission.
- **The full catalog is published as supplementary machine-readable tables with the online version of the article.** [1]

Shape Distribution

Building upon the work of McNeill et al. (2019) [2] we used this extended catalogue of sparse photometry to estimate the shape distribution of NEOs within this size range. There is a relative dearth of shape models for near-Earth objects (NEOs) - only 27 NEAs have shapes obtained from light curve inversion with a further 50-60 from radar observations. Therefore, the best method of obtaining a shape distribution for an overall population remains statistical analysis of sparse photometry and partial light curves.

The result obtained from the expanded sample was statistically identical to the prior result with reduced uncertainties with a mean axis ratio of $\frac{b}{a} = 0.73 \pm 0.04$. This result remains in alignment with past results for NEOs from Pan-STARRS [ibid.] and suggests an increased elongation among small NEOs as compared to kilometer-sized main-belt asteroids. To date, no similar shape distribution for main belt asteroids in the sub-kilometer size regime has been derived however this result is expected in an upcoming publication by the DECam Ecliptic Exploration Project (DEEP).

Cohesive Strength Limits on NEOs

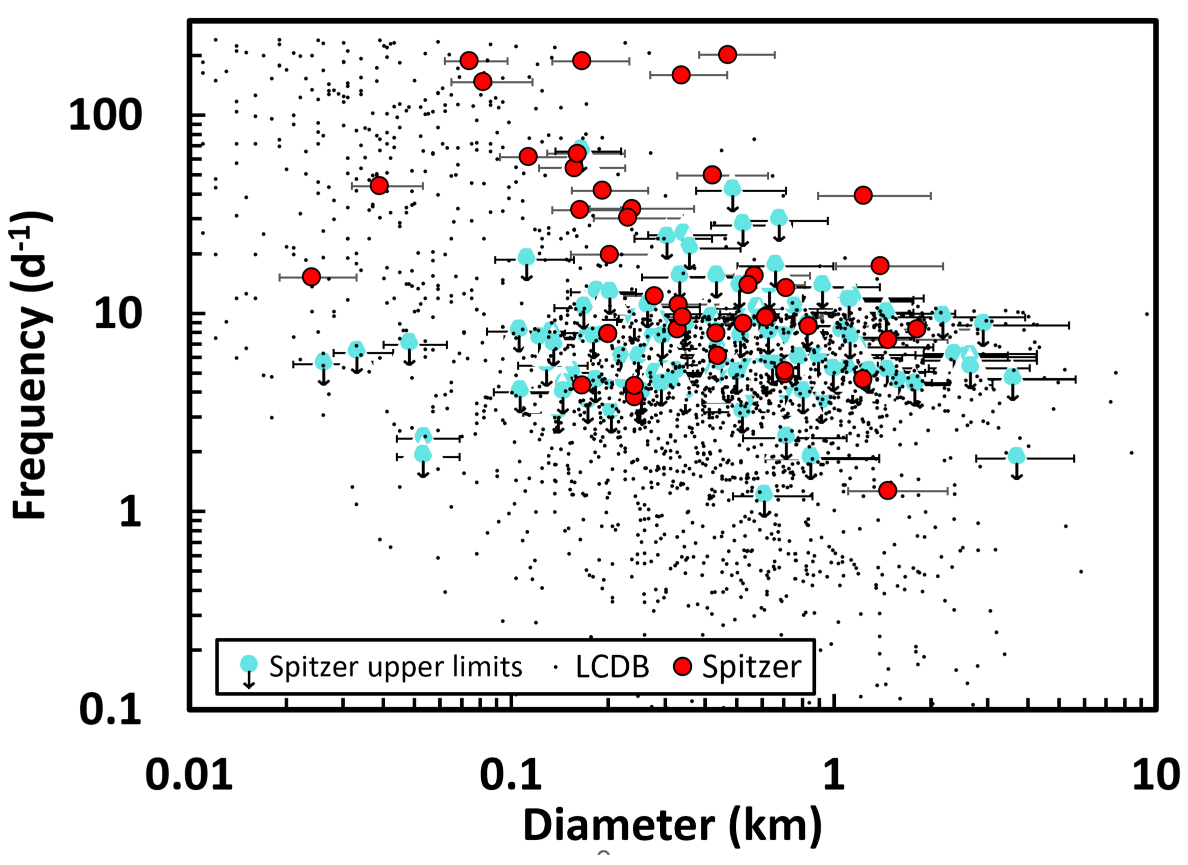

Figure 1 : NEO periods as a function of derived diameter. Black points are data from the Lightcurve Database [6]. Red and blue points are periods and upper limits on period from this work.

For 19 objects with diameters greater than 200m and whose light curves display significant amplitude and/or "super-fast" rotation (P < 2.2 h) we derive the minimum cohesive strength required for these objects to resist rotational fission - an example light curve for one such object is given as Figure 2. Most of these results fall in the tens to hundreds of Pascals range which is in keeping with previous studies [4].

Applying a cut for false-alarm probability (FAP) leaves eleven objects requiring internal cohesive strength - these are presented in Table 1. Without formal taxonomic classification for these objects, we use the derived geometric albedo for these objects to assign an estimated density of 1700 or 2500 $\mathrm{kg\ m^3}$ for albedo lower or higher, respectively, than 0.10.

We calculate a significantly larger strength for the potentially hazardous asteroid 2002 TW55. Sufficiently so that it suggests an increased likelihood that the object is monolithic rather than an aggregate, however the FAP was above our threshold so it is excluded here. Despite this, the nature of this object merits further observations in the future.

Table 1. Summary of Objects Requiring Cohesive Strength to Resist Fission

Object	ρ (kg m^{-3})	Cohesive Str.(Pa)
2000 DP107	1700	11^{+2}_{-4}
2001 UV16	2500	945^{+231}_{-176}
2007 BX48	2500	44^{+14}_{-10}
2008 EY68	1700	51^{+13}_{-9}
2009 DR3	1700	46^{+11}_{-7}
2011 LL2	2500	2011^{+728}_{-398}
2011 XA3	2500	75^{+15}_{-12}
2012 BF86	2500	98^{+27}_{-20}
2012 WK4	2500	192^{+58}_{-43}
2013 VO5	2500	151^{+36}_{-43}
Fewer than two periods sampled:		
2006 GU	1700	203^{+43}_{-40}

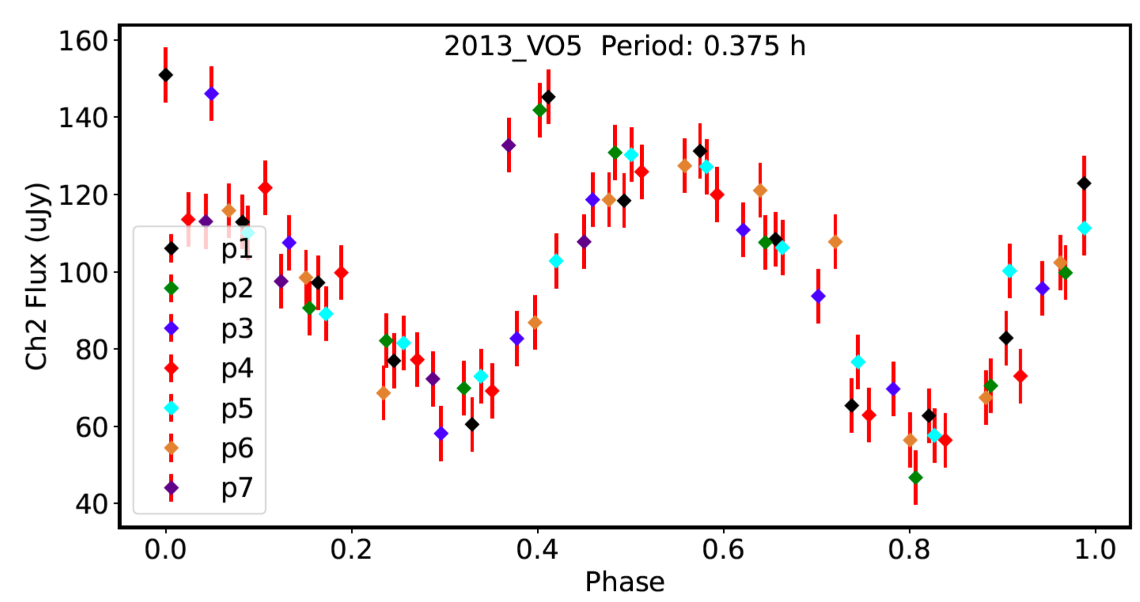

Figure 2 : Spitzer lightcurve for the potentially hazardous asteroid 2013 VO5.

Albedo and Diameter

Spitzer photometric values have been combined with optical magnitudes to fit a thermal model to the NEO and derive estimated diameters and albedos as presented in Figure 3. The lightcurve measurements will allow estimates of the uncertainty of the thermal modeling based on single flux values. These updated diameter values and associated uncertainties derived from the Near-Earth Asteroid Thermal Model also allow for potential reclassification of PHAs as shown in Figure 4. Provisional results are presented here and the full work will be presented in an upcoming publication by Allen et al. [7].

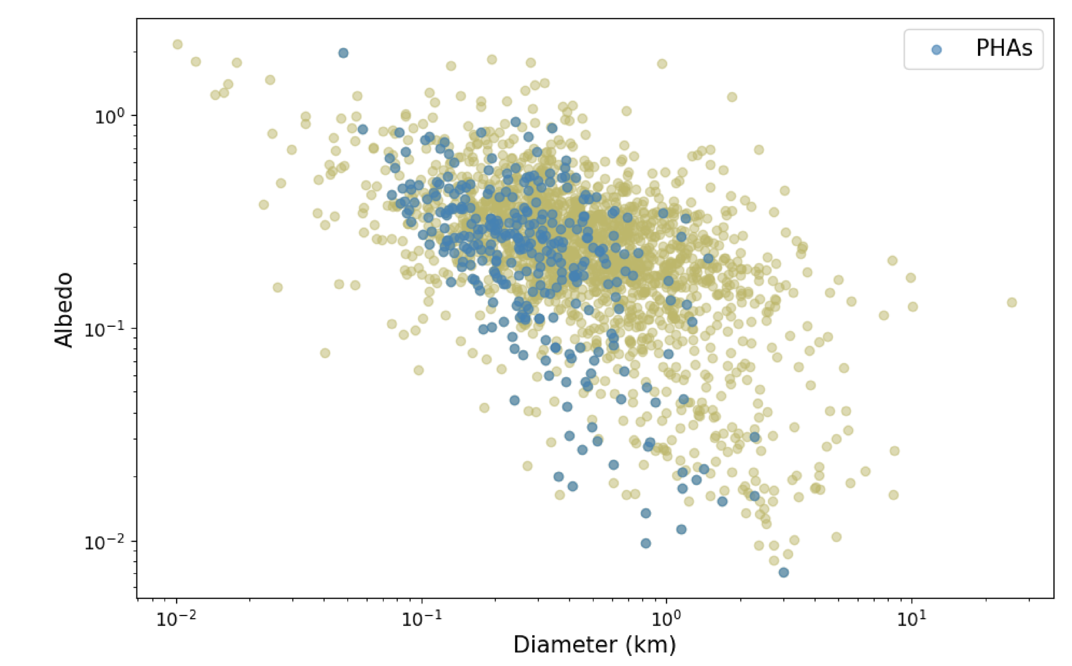

Figure 3 : Albedo vs. Diameter derived for all Near-Earth Objects observed by Spitzer - those objects considered as PHAs are marked as blue data points.

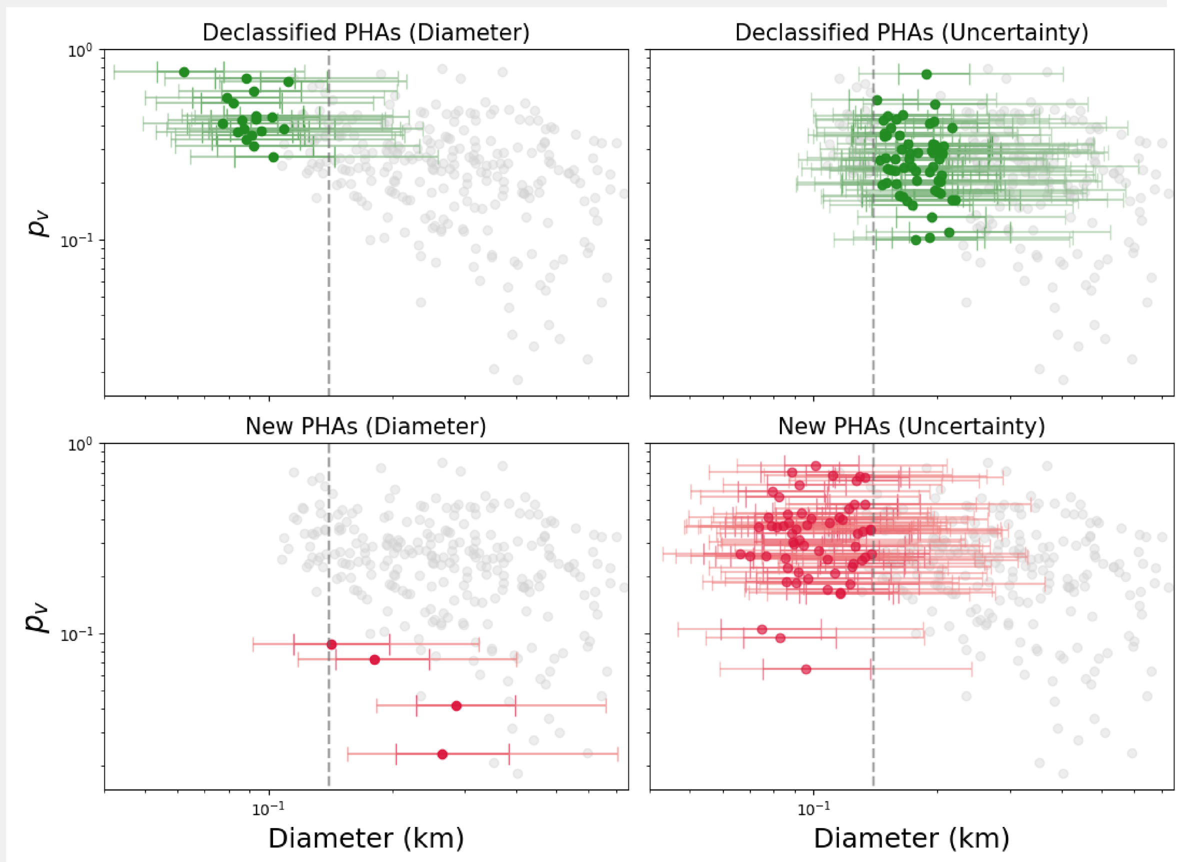

Figure 4 : Objects of interest are colored in green and red. Light gray objects are PHAs whose revised diameters and albedos did not change their classification. The vertical dashed line indicates the 0.14 km diameter threshold for PHA status.

Top left: 20 PHAs with nominal diameters below the threshold.
Top right: 60 PHAs with nominal diameters above the threshold, but minimum uncertainties that dip below it.
Bottom left: 4 non-PHAs whose nominal diameters and orbital parameters meet PHA classification criteria.
Bottom right: 60 non-PHAs with nominal diameters below the threshold, but maximum uncertainties and orbital parameters meeting PHA criteria.

References

[1] J. L. Hora, A. Allen, D. E. Trilling, H. Smith, A. McNeill, (2025), AJ, 169, 5, 256
[2] A. McNeill, J. L. Hora et al., (2019), AJ, 157, 164.
[3] A. Allen, D. Trilling, J. Hora et al. AAS/DPS Abstracts 55, p. 412.07
[4] R. Strauss, A. McNeill, D. E. Trilling et al., (2024), AJ, 168, 184
[5] D.E. Trilling et al. (2024), AJ, 167, 3, 132 [6] B. Warner, A.W. Harris, P.Pravec, Icarus, Volume 202, Issue 1, p. 134-146.
[7] A. Allen, D. Trilling, J. Hora, (2025; in prep.)

mcneia@bgsu.edu, aa5263@nau.edu